

## Effect of Ancillary Ligands on the Reactivity and Structure of Zinc Polysulfido Complexes

Robert J. Pafford and Thomas B. Rauchfuss\*

School of Chemical Sciences, University of Illinois, Urbana, Illinois 61801

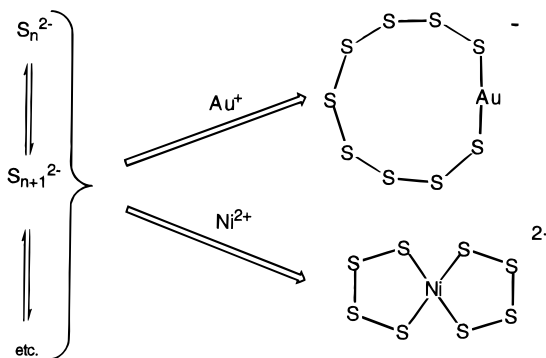
Received December 12, 1997

The pentacoordinate complex  $\text{ZnS}_4(\text{PMDETA})$  (**1**) is formed by treatment of  $\text{ZnS}_6(\text{TMEDA})$  (**2**) with the tridentate ligand pentamethyldiethylenetriamine (PMDETA).  $^1\text{H}$  NMR studies show that samples of **1** react with elemental sulfur to produce a significant (<30%) amount of a second polysulfido complex, assigned as  $\text{ZnS}_5(\text{PMDETA})$ . Crystallographic studies reveal that **1** has a  $\text{ZnN}_3\text{S}_2$  coordination sphere with a distorted trigonal bipyramidal structure. The inversion of the stereochemistry at Zn in **1** has been observed by variable-temperature  $^1\text{H}$  NMR spectroscopy. Neither free PMDETA, elemental sulfur, nor  $\text{ZnS}_5(\text{PMDETA})$  affects the coalescence behavior of **1**. The isomerization mechanism proposed for this process involves the dissociation of the central amine, formation of a tetrahedral  $\text{ZnN}_2\text{S}_2$  intermediate, and inversion at the central nitrogen, followed by recoordination of the central amine. Other PMDETA complexes studied in this work are subject to similar dynamics. Reactivity studies indicate that complex **1** is significantly more nucleophilic than the corresponding  $\text{ZnS}_6(\text{TMEDA})$ , the enhanced nucleophilicity being attributed to the influence of the third amine ligand. Complex **1** reacts rapidly at room with dimethyl acetylenedicarboxylate (DMAD) to give the dithiolene complex  $\text{ZnS}_2\text{C}_2(\text{CO}_2\text{Me})_2(\text{PMDETA})$  (**3**). The rate of the DMAD reaction was >100 times faster higher than that for the reaction of  $\text{ZnS}_6(\text{TMEDA})$  with DMAD, indicative of the enhanced nucleophilicity of the sulfur ligands in **1**. As further evidence for the enhanced nucleophilicity of its polysulfido ligand, **1** reacts with other unsaturated species such as  $\text{CS}_2$  and the dithiocarbonate  $\text{C}_2(\text{S}_2\text{CO})_2$  to give  $\text{ZnS}_3\text{CS}(\text{PMDETA})$  and  $\text{Zn}(\text{S}_2\text{C}_2\text{S}_2\text{CO})(\text{PMDETA})$ , respectively. The perthiocarbonate reacts further with  $\text{PPh}_3$  to give  $\text{ZnS}_2\text{CS}(\text{PMDETA})$ .

## Introduction

Coordination compounds with polysulfido ligands are well-known, and the reactivity of these species has been studied for many years.<sup>1</sup> In contrast to other more classical chelating organic ligands, polysulfides are facultative in the sense that they can adjust their chain length to suit the geometric preferences of the host metal. Illustrative of their self-adjusting chain lengths is the formation of the nonasulfido and tetrasulfido complexes,  $\text{AuS}_9^-$  and  $\text{Ni}(\text{S}_4)_2^{2-}$ , from essentially the same polysulfido sources (Scheme 1). Polysulfido ligands differ from classical chelating ligands in a second way: they are reactive, undergoing conversions involving scission of or insertion into S–S bonds. While these two attributes, adjustable chelate ring size and S-centered reactivity, have been recognized for several years, there are few studies probing the relationship among the size of  $\text{MS}_n$  rings, the nature of the coligands, and S-centered reactivity. It is already known that coligands can crowd the coordination sphere about the metal, leading to altered polysulfido chain lengths. This has been demonstrated in the case of  $(\text{C}_5\text{R}_5)_2\text{TiS}_x$ , where, for  $\text{R} = \text{H}$ , the stable chelate ring size is 6 whereas, for  $\text{R} = \text{Me}$ , the stable ring size is 4, cf.  $(\text{C}_5\text{H}_5)_2\text{TiS}_5^{2-}$  and  $(\text{C}_5\text{Me}_5)_2\text{TiS}_3$ ,<sup>3</sup> respectively.<sup>4</sup> It is also logical to expect that the reactivity of polysulfido complexes could be modified through changes in ancillary ligands. This aspect has not been examined previously, but the present work shows that ancillary ligands can have a significant influence on the nucleophilicity of polysulfido ligands.

## Scheme 1



In view of the preceding discussion, it would be especially interesting to compare the structures and reactivities of species of the types  $\text{MS}_x\text{L}_2$  and  $\text{MS}_y\text{L}_3$  for a given M. Studies of this type have not been conducted previously because there are few polysulfido complexes whose coligands can be exchanged. The compounds of the type  $\text{ZnS}_x\text{L}_2$  do however undergo ligand exchange as illustrated by the conversion of  $\text{ZnS}_6(\text{py})_2$  to  $\text{ZnS}_6(\text{MeIm})_2$ , where py is pyridine and MeIm is *N*-methylimidazole.<sup>5</sup> Trends in substitution reactions mirror the Bronsted basicity of the amine. Previous studies on this equilibrium did not probe the effect of multidentate ligands, which might alter the coordination number at Zn.

## Results

**Synthesis and Structure of  $\text{ZnS}_4(\text{PMDETA})$ .** Solutions of  $\text{ZnS}_6(\text{TMEDA})^3$  react at room temperature with a slight excess

(1) Draganjac, M. E.; Rauchfuss, T. B. *Angew. Chem., Int. Ed. Engl.* **1985**, *24*, 742.

(2) Samuel, E. *Bull. Soc. Chim. Fr.* **1966**, *64*, 3548.

(3) Shaver, A.; McCall, J. M. *Organometallics* **1984**, *3*, 1823.

(4) A similar situation applies to  $\text{Cp}^*_2\text{VS}_2$  (Koch, S. A.; Chebolu, V. *Organometallics* **1983**, *2*, 350) vs  $\text{Cp}^*_2\text{VS}_5$  (Köpf, H.; Kahl, W.; Wirl, A. *Angew. Chem., Int. Ed. Engl.* **1970**, *9*, 801).

(5) Verma, A. K.; Rauchfuss, T. B.; Wilson, S. R. *Inorg. Chem.* **1995**, *34*, 3072. Verma, A. K.; Rauchfuss, T. B. *Inorg. Chem.* **1995**, *34*, 6199. Verma, A. K. Ph.D. Thesis, University of Illinois at Urbana-Champaign, 1996.

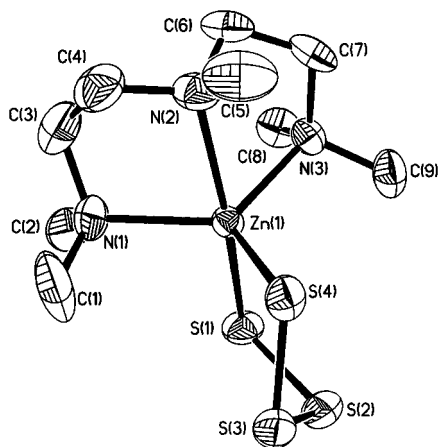


**Figure 1.** ORTEP view of the non-hydrogen atoms of  $\text{ZnS}_4(\text{PMDETA})$  (**1**) with thermal ellipsoids set at 50%.

**Table 1.** Selected Distances (Å) and Bond Angles (deg) for Compounds **1** and **3**

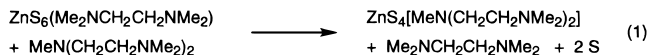
	<b>1</b>	<b>3</b>
Zn1–N1	2.185(3)	2.188(3)
Zn1–N2	2.312(3)	2.347(3)
Zn1–N3	2.176(2)	2.140(3)
Zn1–S1 <sup>a</sup>	2.4389(8)	2.3744(12)
Zn1–S4(2) <sup>b</sup>	2.3550(7)	2.3141(11)

	<b>1</b>	<b>3</b>
N1–Zn1–N3	123.06(10)	118.64(13)
N1–Zn1–N2	79.56(11)	78.44(13)
N2–Zn1–N3	79.75(9)	80.66(12)
N1–Zn1–S1	93.38(9)	96.66(10)
N2–Zn1–S1	166.26(8)	174.74(9)
N3–Zn1–S1	94.62(7)	100.27(10)
N1–Zn1–S4(2)	116.44(8)	119.22(10)
N2–Zn1–S4(2)	93.17(8)	91.85(9)
N3–Zn1–S4(2)	117.15(6)	118.48(9)
S1–Zn1–S4(2)	100.54(3)	92.23(4)

<sup>a</sup> S1–S2 = 2.0613(13), S2–S3 = 2.0477(13), S3–S4 = 2.0672(13) Å. <sup>b</sup> The numbering systems for the S atoms differ for the two structures. For compound **1**, S1 and S4 are coordinated while, for **3**, S1 and S2 are coordinated.

of the triamine *N,N,N',N''*-pentamethyldiethylenetriamine (PMDETA). Bright yellow crystals of  $\text{ZnS}_4(\text{PMDETA})$  (**1**) can be precipitated from MeCN solution using ether (eq 1).



Microcrystalline samples of **1** are air stable for days. Over long periods, samples of **1** decompose in air to give products that have strong IR bands in the 1150–1200  $\text{cm}^{-1}$  region, indicative of the thiosulfate group.<sup>5,6</sup>

Crystallographic analysis of **1** reveals that the zinc is five coordinate with a  $\text{N}_3\text{S}_2$  coordination sphere (Figure 1, Table 1). The coordination geometry about the zinc is distorted trigonal bipyramidal; the amine ligands occupy the face with the central amine located at one apex of the trigonal bipyramid. The  $\text{ZnN}_2\text{C}_2$  rings of the PMDETA ligand adopt a  $\delta,\delta$  configuration.<sup>7</sup> The  $\delta,\lambda$  isomer is not present in the lattice although both almost certainly coexist in solution. Deviation from idealized trigonal bipyramidal geometry is indicated by

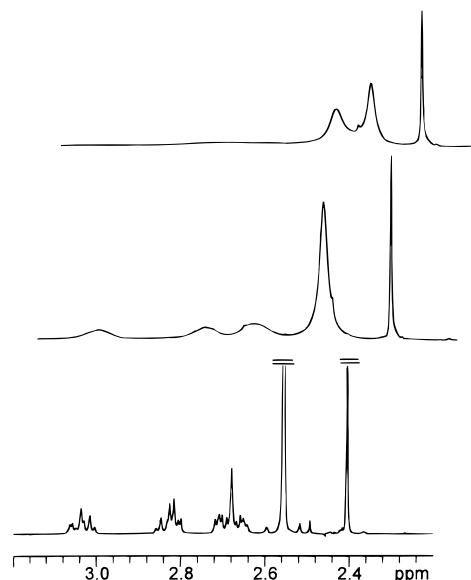
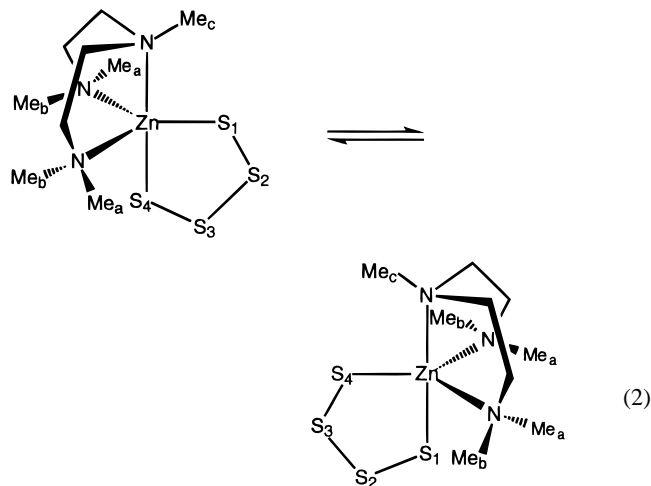


**Figure 2.** 500 MHz  $^1\text{H}$  NMR spectra for  $\text{ZnS}_4(\text{PMDETA})$  (**1**) (acetone- $d_6$  solvent) recorded at 22 (bottom),  $-40$  (middle), and  $-60$  °C (top).

the fact that the N2–Zn–S1 angle is  $166.26(8)^\circ$ . This distortion is partially attributable to the rather wide S–Zn–S ( $100.55(3)^\circ$ ) angle demanded by the tetrasulfide, which spans axial and equatorial sites. The terminal amines on the PMDETA form shorter Zn–N bonds ( $\sim 2.18$  Å) than the central amine (2.31 Å). This has been seen in other PMDETA complexes.<sup>8,9</sup>

The solution structure of **1** was also studied using  $^1\text{H}$  DNMR spectroscopy. At room temperature, one observes two methyl signals in a 4:1 ratio. On the basis of the structures shown in eq 2, we might have expected the pattern for methyl signals to



be 2:2:1. Two of the methyl signals indeed split into a 2:2:1 set of singlets at low temperatures (Figure 2). This pattern is consistent with inversion of stereochemistry at Zn, which proceeds via inversion of the central NMe center and results in equivalencing of the diastereotopic NMe<sub>2</sub> groups.

**Studies on  $\text{ZnS}_x(\text{PMDETA})$  ( $x \neq 4$ ) and  $\text{ZnS}_y(\text{TMEDA})$  ( $y \neq 6$ ).** The  $^1\text{H}$  NMR spectrum of some samples of **1** revealed the presence of a second PMDETA complex which exists at concentrations up to 20% of **1**, based on integrated  $^1\text{H}$  NMR

(6) Nakamoto, K. *Infrared and Raman Spectra of Inorganic and Coordination Compounds*; Wiley: New York, 1986; p 252.

(7) Hawkins, C. J.; Palmer, J. A. *Coord. Chem. Rev.* **1982**, *44*, 1.

(8) Synthesis, spectroscopy, and structure of  $\text{MCl}_2(\text{PMDETA})$ : Di Vaira, M.; Orioli, P. L. *Inorg. Chem.* **1969**, *8*, 2729. Ciampolini, M.; Speroni, G. P. *Inorg. Chem.* **1966**, *5*, 45.

(9) Koutsantonis, G. A.; Lee, F. C.; Raston, C. L. *J. Chem. Soc., Chem Commun.* **1994**, 1975.

intensities. This minor component is innocuous in terms of other reactivity studies (see below). Spectroscopically pure samples of **1** can be obtained by crystallization from neat PMDETA, possibly reflecting the relatively high solubility of  $S_8$  in this medium vs MeCN, the usual solvent for the conversion of  $ZnS_6$ (TMEDA) into **1**. The second component is formed upon the addition of excess elemental sulfur to solutions of pure **1**. The collected evidence points to the conclusion that the minor component is a higher polysulfide such as  $ZnS_5$ (PMDETA) or  $ZnS_6$ (PMDETA) (eq 3). Furthermore, the minor component

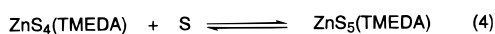


disappears upon addition of  $PPh_3$  to solutions of **1**. The addition of  $PBu_3$  also removes the minor component from solutions of **1**, but this more potent S-abstracting agent also leads to some decomposition, as evidenced by the appearance of free PMDETA. The presence of  $ZnS_5$ (PMDETA) does not affect the dynamic NMR properties of **1** up to 70 °C. This indicates that intermetallic S atom exchange is relatively slow. On the basis of the equilibrium shown in eq 3, one would expect that the ratio  $ZnS_4$ (PMDETA)/ $ZnS_5$ (PMDETA) would be independent of  $[ZnS_x(PMDETA)]_{total}$  provided that  $[S_8]$  is constant, as for solutions saturated in elemental sulfur:

$$\frac{[ZnS_5(PMDETA)]}{[ZnS_4(PMDETA)]} = K_{eq}[S_8]^{1/8}$$

This condition was observed by serial dilution of  $S_8$ -saturated solutions of **1** in MeCN.

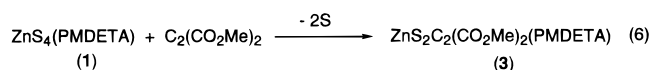
In view of the evidence that **1** binds sulfur to form a second polysulfido complex, we reinvestigated the recently reported<sup>3</sup>  $ZnS_6$ (TMEDA) (**2**). We reconfirmed the  $^1H$  NMR data for **2** in pyridine and  $CH_2Cl_2$  solutions, which indicate a single species. In MeCN solutions, however, it is obvious that there are *three* TMEDA complexes in a ratio of 1:1.5:12 (eqs 4 and 5). Evaporation of the solution and redissolution in  $CH_2Cl_2$



give the original simple spectrum. The ratio of the three species can be shifted toward the minor species by the addition of  $PPh_3$  to these solutions. This shows that these minor species are less S-rich than the original hexasulfido complex. Over time, however, such solutions revert to the same (1:1.5:12) equilibrium ratio concomitant with the formation of free TMEDA. Addition of sulfur to MeCN solutions of **2** does not affect the equilibrium ratio.

#### Reactions of $ZnS_4$ (PMDETA) with Electrophilic Alkynes.

The reaction of metal polysulfido complexes with the electrophilic alkyne DMAD provides a means to evaluate the relative nucleophilicity of the polysulfido compound.<sup>10</sup> Complex **1** reacts very rapidly with dimethyl acetylenedicarboxylate (DMAD) to give the dithiolene  $ZnS_2C_2(CO_2Me)_2$ (PMDETA) (**3**) (eq 6).



This reaction occurs in seconds at room temperature. In

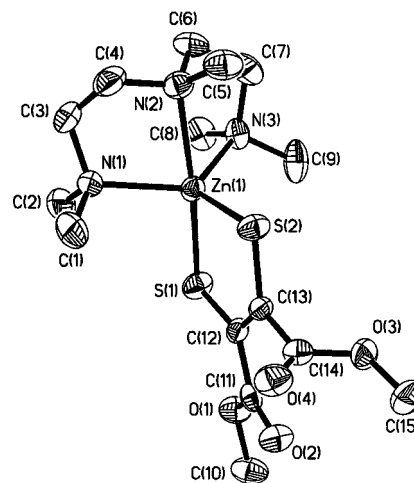


**Figure 3.** ORTEP view of the non-hydrogen atoms of  $ZnS_2C_2(CO_2Me)_2$ (PMDETA) (**3**) with thermal ellipsoids set at 50%.

contrast, the reaction of  $ZnS_6$ (TMEDA) with DMAD requires several hours to reach completion.<sup>3</sup>

Solutions of **1** also react with methyl propiolate,  $MeO_2CC_2H$ , to give the unsymmetrical dithiolene  $Zn[S_2C_2(CO_2Me)H]$ (PMDETA) (**4**). Consistent with the diminished electrophilicity of this alkyne, it reacts more slowly with **1** than does DMAD. We showed that, under comparable conditions, the rate of reaction of **1** with methyl propiolate was >100 times faster than the reaction of **2** with the same substrate.

The crystallographic analysis revealed that, like **1**, **3** is pentacoordinate with a  $N_3S_2$  coordination sphere (Figure 3, Table 1).<sup>11</sup> The coordination geometry about the zinc is distorted trigonal bipyramidal; the amine ligands occupy the face with the central amine located at one apex of the trigonal bipyramid. In the solid-state structure of **3**, the  $ZnN_2C_2$  rings adopt both the  $\delta,\delta$  and  $\lambda,\lambda$  conformations. Similar to the case of **1**, deviation from an idealized tbp is indicated by the fact that the  $N2-Zn-S1$  angle is  $174.74(9)^\circ$ , vs the idealized value of  $180^\circ$ . The angle here is closer than the  $166.26(8)^\circ$  seen for the  $S_4$  complex. This is partially attributed to the smaller chelate angle for the dithiolene ( $S-Zn-S = 92.23(4)^\circ$ ) versus the  $S_4$  ( $S-Zn-S = 100.55(3)^\circ$ ). Furthermore, the average  $Zn-S$  distances are shorter in the dithiolene **3** (2.3141(11) and 2.3744(12) Å) than in **1** (2.3550(7) and 2.4389(8) Å). As was seen for the  $S_4$  complex, the terminal amines on the PMDETA ligand form shorter  $Zn-N$  bonds (2.140(3) and 2.188(3) Å) than the middle amine ( $r(Zn-N2) = 2.347(3)$  Å).

Variable-temperature NMR studies of **3** were of interest since the dithiolene methyl signals provide insights into the dynamics of the  $ZnS_2C_2(CO_2Me)_2$  moiety relative to the PMDETA fragment, information that was not available from studies on **1**. Low-temperature NMR studies show that the 4:1 patterns for the methyl signals of the PMDETA ligand split into a 2:2:1 set of singlets (Figure 4). Concomitantly, the  $CO_2CH_3$  signals split into a 1:1 pattern. These observations are consistent with a mechanism where pyramidalization of the central NMe center is coupled to the inversion of stereochemistry at Zn (eq 7).

**Reaction of  $ZnS_4$ (PMDETA) with  $CS_2$  and Related Reactions.** Consistent with its enhanced nucleophilicity, **1** is reactive toward  $CS_2$ . Solutions of **1** in MeCN rapidly darken upon exposure to stoichiometric amounts of  $CS_2$  concomitant with

(10) Bolinger, C. M.; Rauchfuss, T. B. *Inorg. Chem.* **1982**, *21*, 3947. Bolinger, C. M.; Rauchfuss, T. B.; Wilson, S. R. *J. Am. Chem. Soc.* **1981**, *103*, 5620.

(11) Other pentacoordinated zinc dithiolenes: Zhang, C.; Chadha, R.; Reddy, H. K.; Schrauzer, G. N. *Inorg. Chem.* **1991**, *30*, 3865.

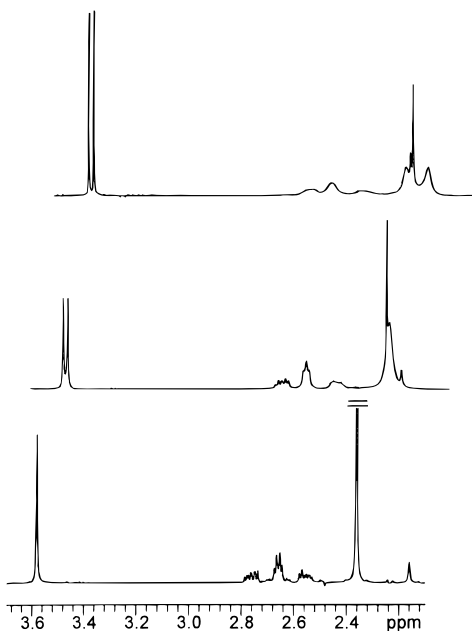
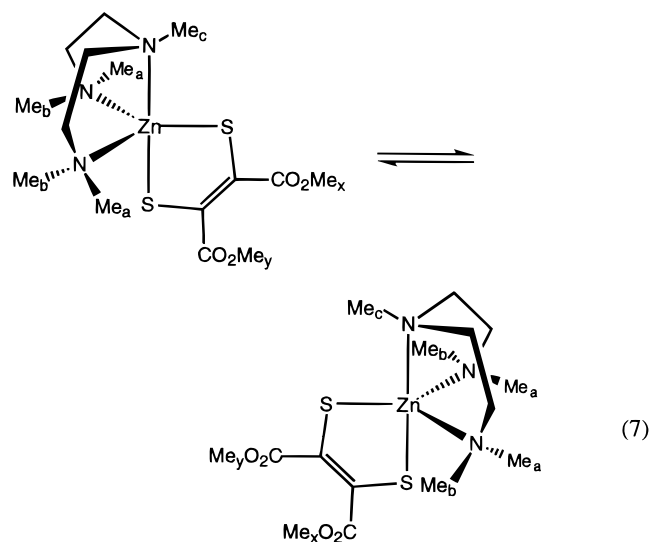
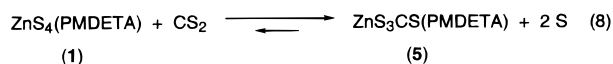


**Figure 4.** 500 MHz  $^1\text{H}$  NMR spectra of  $\text{ZnS}_2\text{C}_2(\text{CO}_2\text{Me})_2(\text{PMDETA})$  (**3**) ( $\text{CD}_3\text{CN}$  solvent) recorded at 22 (bottom),  $-20$  (middle), and  $-40$   $^\circ\text{C}$  (top).

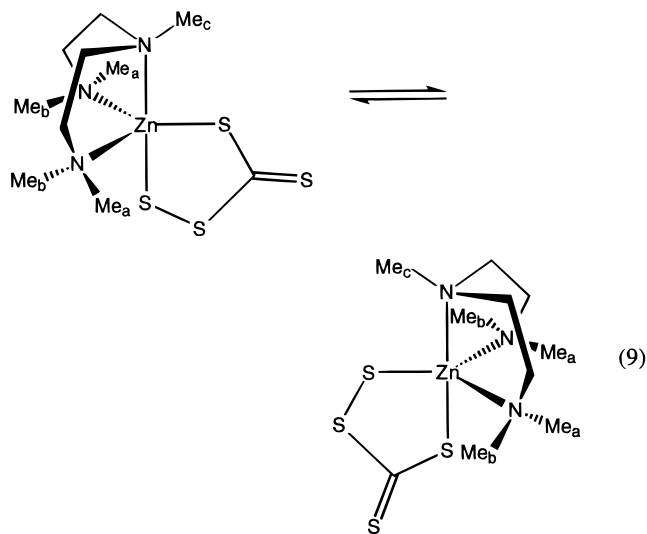


the precipitation of elemental sulfur (eq 8).  $^1\text{H}$  NMR analysis



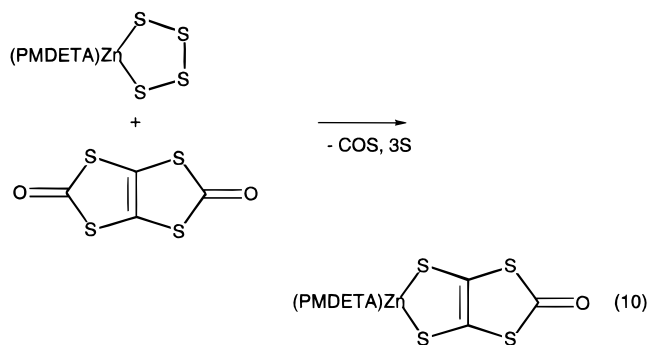
of the reaction products showed that crude samples of the new compound contain  $\sim 35\%$  unreacted **1**. Addition of further  $\text{CS}_2$  to such solutions shifts the equilibrium toward **5**. One can prepare analytically pure **5** through multiple extraction of crude samples of **5** with  $\text{CS}_2$ . Solutions of **5** are stable for days and show no sign of decomposition by NMR spectroscopy; i.e., there is no evidence that **3** serves as a precursor to “ $\text{ZnS}_2(\text{PMDETA})$ ”, via the thermal elimination of  $\text{CS}_2$ . Note that **2** does not react with  $\text{CS}_2$ .

The DNMR properties of **5** were of interest since the chelating sulfur ligand is unsymmetrical (eq 9). The room-temperature  $^1\text{H}$  NMR spectrum of **5** is slightly broadened due to chemical exchange. As in other cases examined in this work, the dynamics are intramolecular since the addition of  $\text{CS}_2$  to these solutions did not influence the line broadening. At  $-40$   $^\circ\text{C}$ ,



the  $^1\text{H}$  NMR spectrum consists of *two* sets of 2:2:1 singlets, in approximately equal abundance. This is consistent with two isomers that differ with regard to the relative position of the thiocarbonyl center (Figure 5). The addition of  $\text{PPh}_3$  to a solution of **5** gave the pale yellow trithiocarbonate  $\text{ZnS}_2\text{CS}(\text{PMDETA})$  (**6**). This process can be reversed by the addition of  $\text{S}_8$  to solutions of **6**.

In an extension of the addition of cumulenes to **1**, we examined the electrophilic dithiocarbonate tetrathiapentalenedione (TPD). This species is known to convert anionic metal sulfido compounds into dithiolenes.<sup>12</sup> The heterocycle rapidly reacts with **1** to give the dithiolene  $\text{ZnS}_2\text{C}_2\text{S}_2\text{CO}(\text{PMDETA})$  (**7**) (eq 10).



## Discussion

Prior to our studies, there had been some significant work on zinc polysulfido complexes. The tetrahedral complexes  $\text{Zn}(\text{S}_x)_2^{2-}$  ( $x = 4-6$ ) have been characterized crystallographically. Coucouvanis and co-workers showed that these complexes can be interconverted using the S-abstracting agent  $\text{PPh}_3$  and the S atom donor  $(\text{PhCH}_2\text{S})_2\text{S}$ . Additionally these anionic complexes were shown to add both  $\text{CS}_2$  and the activated alkyne DMAD to give  $\text{Zn}(\text{CS}_4)_2^{2-}$  and  $\text{Zn}[\text{S}_2\text{C}_2(\text{CO}_2\text{Me})_2]_2^{2-}$ , respectively.<sup>13</sup> As discussed below, the reactivity of **1** is more similar to that of an anionic zinc polysulfido complex, not  $\text{ZnS}_6(\text{TMEDA})$ .

(12) Yang, X.; Freeman, G. K. W.; Rauchfuss, T. B.; Wilson, S. R. *Inorg. Chem.* **1991**, *30*, 3034.

(13) Coucouvanis, D.; Patil, P. R.; Kanatzidis, M. G.; Detering, B.; Baenziger, N. C. *Inorg. Chem.* **1985**, *24*, 24. Müller, A.; Schimanski, J.; Schimanski, U.; Bögge, H. Z. *Naturforsch.* **1985**, *40B*, 1277.

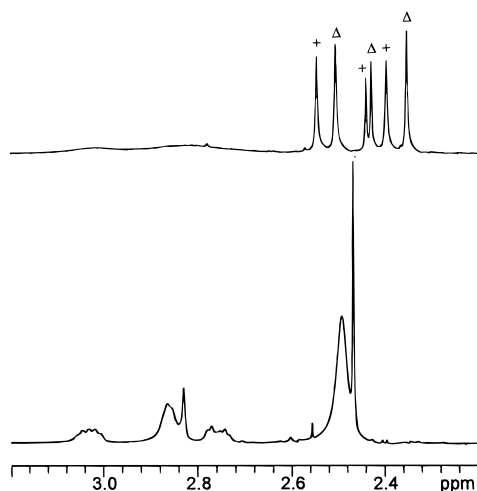
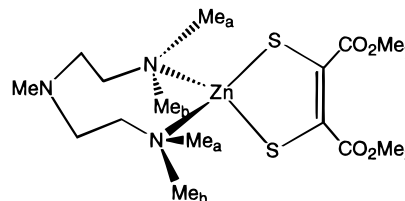


**Figure 5.** 500 MHz  $^1\text{H}$  NMR spectra of  $\text{ZnS}_3\text{CS(PMDETA)}$  (**5**) (acetone- $d_6$  solvent) recorded at 22 (bottom) and  $-40$  °C (top).

With regard to its structure, compound **1** is mainly of interest because of the influence of the amine on the length of the polysulfido chain. Solution studies are particularly informative since we observed that both **1** and **2** exist as equilibrium mixtures; the ratio of the components can be shifted by the addition or removal of sulfur. The TMEDA complex consists primarily of a hexasulfide while the PMDETA complex consists mainly of the tetrasulfide. This trend indicates that higher coordination numbers lead to decreased S–M–S angles, which in turn favors fewer S atoms in the polysulfide chain. In general, the size of a polysulfido chelate rings is related to the Cl–M–Cl angle in the corresponding  $\text{MCl}_2\text{L}_n$  complex; e.g., tetrahedral polysulfido complexes tend to have longer chain lengths than corresponding square planar complexes. It seems quite likely that equilibria similar to the one observed in this work apply to other polysulfido complexes, but the lack of convenient spectroscopic probes (e.g., NMR spectroscopy) has limited insights into such equilibria. Equilibria involving different lengths of polysulfido ligands have been observed previously for  $\text{Cp}^*\text{Ir}(\text{PMe}_3)_x\text{S}_x$ , where  $x = 4$ – $6$ ,<sup>14</sup>  $\text{IrS}_{18}^{3-}$ ,<sup>15</sup> and  $\text{Pt}(\text{S}_x)_3^{2-}$  where  $x = 5, 6$ .<sup>16</sup> These equilibria can be shifted by removal of sulfur from or the addition of sulfur to the solutions.  $^{113}\text{Cd}$  NMR measurements have provided evidence for  $[\text{Cd}(\text{S}_x)(\text{S}_y)]^{2-}$  ( $x = 5, 6$ ;  $y = 5$ – $7$ ),<sup>17</sup> while  $^{199}\text{Hg}$  NMR measurements have indicated the interconversion of  $[\text{Hg}(\text{S}_x)(\text{S}_y)]^{2-}$ , where  $x = 4, 5$  and  $y = 4$ – $6$ .<sup>18</sup> There has also been extensive work on the ring contraction reactions of the main group tetrasulfides  $\text{Ar}_2\text{ES}_4$  ( $\text{E} = \text{Si}, \text{Ge}, \text{Sn}, \text{Pb}$ ), but equilibria involving different chain lengths have not been observed in these systems.<sup>19</sup>

The PMDETA ligand lends itself to detailed analysis of the stereochemistry of its complexes. At higher temperatures, we observed equivalencing of the diastereotopic  $\text{NMe}_2$  groups. The inversion of tertiary amines typically is subject to very low barriers;<sup>20</sup> thus the much higher barriers indicated in this work ( $\sim 50$  kJ/mol) reflect the strength of the Zn–N bond, since amine inversion occurs only after dissociation of the Zn–N bond. We observe that the interconversion of the diastereotopic  $\text{NMe}_2$  groups occurs in the same temperature range as the decoalescence of the methyl ester signals in dithiolene **3**. We conclude that these two coalescence patterns result from the inversion of stereochemistry at zinc. We propose that this stereodynamic process is initiated by dissociation of the Zn–NMe bond followed by formation of a tetrahedral  $\text{ZnN}_2\text{S}_2$  intermediate:



The fact that the central amine linkage to Zn is longer in these complexes is also consistent with the proposal that inversion of stereochemistry at zinc is initiated by dissociation of this bond. Evidence for a second dynamic process was obtained at  $-90$  °C, where the  $^1\text{H}$  NMR signals for the methyl groups on PMDETA begin to split further and triplets appear for the methylene groups of the chelate backbone. We assume that we are observing the onset of the slow interconversion of  $\delta$  and  $\lambda$  conformers of the chelate ring.<sup>7,21</sup>

The nucleophilicity<sup>22</sup> of  $\text{ZnS}_4(\text{PMDETA})$  is noticeably enhanced relative to that of  $\text{ZnS}_6(\text{TMEDA})$ . This fact was established through the reactions of **1** with DMAD and  $\text{CS}_2$ . The diamine complex  $\text{ZnS}_6(\text{TMEDA})$  reacts  $\sim 100$  times more slowly with DMAD and is completely unreactive toward  $\text{CS}_2$ . Thus, it is clear that the third amine strongly enhances the nucleophilicity of **1**.

## Experimental Section

Synthetic operations were performed under a dinitrogen atmosphere using standard Schlenk-line techniques, unless mentioned otherwise. PMDETA was distilled from KOH at 1 atm. Tetrathiapentalenedione (TPD) was prepared by literature methods.<sup>23</sup>

The following instruments were employed: a Mattson Galaxy Series 3000 FTIR spectrometer and a Rigaku D-Max powder X-ray diffractometer with Cu target (X-ray diffraction). Solution NMR spectra were recorded with Varian NMR U400 and U500 spectrometers operating at 400 and 500 MHz, respectively. Chemical shifts are reported in ppm vs TMS ( $\delta$  scale). Microanalyses were performed by the School of Chemical Sciences Microanalytical Laboratory.

**ZnS<sub>4</sub>(PMDETA) (1).** A suspension of 0.405 g (1.083 mmol) of  $\text{ZnS}_6(\text{TMEDA})$  in 10 mL of PMDETA was stirred at room temperature. After 4 h, the suspension was diluted with 30 mL of  $\text{Et}_2\text{O}$  to give a yellow precipitate, which was filtered off and washed with three 15 mL portions of  $\text{Et}_2\text{O}$ . The crude product was then extracted into 10 mL of MeCN, and the solution was filtered. The filtrate was diluted with 50 mL of  $\text{Et}_2\text{O}$ , and the resulting solution was cooled at  $-25$  °C for 3 h. The precipitate was filtered off, washed with  $3 \times 10$  mL of

(14) Herberhold, M.; Jin, G.-X.; Rheingold, A. L. *Chem. Ber.* **1991**, *124*, 2245.

(15)  $\text{Ir}(\text{S}_6)_2(\text{S}_4)^{3-}$ : Albrecht-Schmitt, T. E.; Ibers, J. A. *Angew. Chem., Int. Ed. Engl.* **1997**, *36*, 2010.  $\text{Ir}(\text{S}_6)_3^{3-}$ : Albrecht-Schmitt, T. E.; Ibers, J. A. *Inorg. Chem.* **1996**, *35*, 7273.

(16)  $\text{Pt}(\text{S}_5)_3^{2-}$ : Jones, P. E.; Katz, L. *Acta Crystallogr., Sect. B* **1969**, *25*, 745.  $\text{Pt}(\text{S}_6)_2(\text{S}_5)^{2-}$ : Gillard, R. D.; Wimmer, F. L.; Richards, J. P. G. *J. Chem. Soc., Dalton Trans.* **1985**, 253.

(17) Banda, H. R. M.; Dance, I. G.; Bailey, T. D.; Craig, D. C.; Scudder, M. L. *Inorg. Chem.* **1989**, *28*, 1862.

(18) Bailey, T. D.; Banda, H. R. M.; Craig, D. C.; Dance, I. G.; Ma, I. N. L.; Scudder, M. L. *Inorg. Chem.* **1991**, *30*, 187.

(19) Suzuki, H.; Tokitoh, N.; Nagase, S.; Okazaki, R. *J. Am. Chem. Soc.* **1994**, *116*, 11578 (Si). Matsumoto, T.; Tokitoh, N.; Okazaki, R.; Goto, M. *Organometallics* **1995**, *14*, 1008 (Ge). Matsuhashi, Y.; Tokitoh, N.; Okazaki, R. *Organometallics* **1993**, *12*, 1351 (Sn). Tokitoh, N.; Kano, N.; Shibata, K.; Okazaki, R. *Organometallics* **1995**, *14*, 3121 (Pb).

(20) Lambert, J. B. *Top. Stereochem.* **1971**, *6*, 19.

(21) The barrier for the inversion of the chelate ring in  $\text{ZnCl}_2(\text{TMEDA})$  is estimated to be  $\sim 40$  kJ/mol: Caulton, K. G. *Inorg. Nucl. Chem. Lett.* **1973**, *9*, 533.

(22) Other studies on nucleophilic pentacoordinated Zn–N–S complexes: Wilker, J. J.; Lippard, S. J. *Inorg. Chem.* **1997**, *36*, 969.

(23) Schumaker, R. R.; Engler, E. M. *J. Am. Chem. Soc.* **1977**, *99*, 5521.

**Table 2.** Crystal Data and Structure Refinement Details for Compounds **1** and **3**

	ZnS <sub>4</sub> (PMDETA) ( <b>1</b> )	ZnS <sub>2</sub> C <sub>2</sub> (CO <sub>2</sub> Me) <sub>2</sub> (PMDETA) ( <b>3</b> )
empirical formula	C <sub>9</sub> H <sub>23</sub> N <sub>3</sub> S <sub>4</sub> Zn	C <sub>15</sub> H <sub>29</sub> N <sub>3</sub> O <sub>4</sub> S <sub>2</sub> Zn
formula weight	366.91	444.90
temperature	198(2) K	198(2) K
wavelength	0.710 73 Å	0.710 73 Å
crystal system	orthorhombic	monoclinic
space group	<i>P</i> 2 <sub>1</sub> 2 <sub>1</sub> 2 <sub>1</sub>	<i>P</i> 2 <sub>1</sub> / <i>n</i>
unit cell dimensions	<i>a</i> = 8.34700(10) Å <i>b</i> = 13.7399(2) Å <i>c</i> = 14.3545(3) Å α = 90° β = 90° γ = 90°	8.5096(2) Å 16.3840(5) Å 14.7000(4) Å α = 90° β = 93.8630(10)° γ = 90°
volume, <i>Z</i>	1646.27(5) Å <sup>3</sup> , 4	2044.84(10) Å <sup>3</sup> , 4
density (calculated)	1.480 Mg/m <sup>3</sup>	1.445 Mg/m <sup>3</sup>
absorption coefficient	1.984 mm <sup>-1</sup>	1.429 mm <sup>-1</sup>
<i>F</i> (000)	768	936
crystal size	0.72 × 0.36 × 0.30 mm	0.23 × 0.15 × 0.12 mm
θ range for data collection	2.05 to 28.25°	1.86 to 28.27°
limiting indices	-10 ≤ <i>h</i> ≤ 10, -13 ≤ <i>k</i> ≤ 18, -18 ≤ <i>l</i> ≤ 18	-11 ≤ <i>h</i> ≤ 11, -21 ≤ <i>k</i> ≤ 19, -19 ≤ <i>l</i> ≤ 14
collection method	CCD area detector frames	CCD area detector frames
no. of reflections collected	10 715	13 172
no. of independent reflections	3923 ( <i>R</i> <sub>int</sub> = 0.0391)	4900 ( <i>R</i> <sub>int</sub> = 0.0645)
max and min transmission	0.99805 and 0.80245	0.98998 and 0.89413
absorption correction	ψ scan	ψ scan
refinement method	full-matrix least-squares on <i>F</i> <sup>2</sup>	full-matrix least-squares on <i>F</i> <sup>2</sup>
data/restraints/parameters	3922/0/154	4886/0/226
goodness-of-fit on <i>F</i> <sup>2</sup>	1.022	1.162
final <i>R</i> indices [ <i>I</i> > 2σ( <i>I</i> )] <sup>a</sup>	<i>R</i> <sub>1</sub> = 0.0282, <i>wR</i> <sub>2</sub> = 0.0762	<i>R</i> <sub>1</sub> = 0.0588, <i>wR</i> <sub>2</sub> = 0.0854
<i>R</i> indices (all data) <sup>a</sup>	<i>R</i> <sub>1</sub> = 0.0299, <i>wR</i> <sub>2</sub> = 0.0783	<i>R</i> <sub>1</sub> = 0.1102, <i>wR</i> <sub>2</sub> = 0.1069
largest diff peak and hole	0.730 and -0.520 e <sup>-</sup> Å <sup>-3</sup>	0.460 and -0.370 e <sup>-</sup> Å <sup>-3</sup>

$$^a w = 1/[\sigma^2(F_o^2) + (0.0000P)^2 + 3.6855P], \text{ where } P = (F_o^2 + 2F_c^2)/3.$$

Et<sub>2</sub>O, and dried under vacuum to afford yellow microcrystals. Yield: 0.370 g (93%). Anal. Calcd for C<sub>9</sub>H<sub>23</sub>N<sub>3</sub>S<sub>4</sub>Zn: C, 29.46; H, 6.32; N, 11.45; S, 34.95; Zn, 17.82. Found: C, 29.44; H, 6.60; N, 11.40; S, 34.75; Zn, 18.10. <sup>1</sup>H NMR (CD<sub>3</sub>CN), δ: 2.83 (m, 2H, CH<sub>2</sub>); 2.72 (m, 2H, CH<sub>2</sub>); 2.60 (m, 4H, CH<sub>2</sub>); 2.50 (s, 12H, CH<sub>3</sub>); 2.36 (s, 3H, CH<sub>3</sub>). IR (KBr): 476 cm<sup>-1</sup> (ν<sub>SS</sub>). A more efficient synthesis of **1** that produced a less pure product involved treatment of a solution of 2.00 g (5.35 mmol) of ZnS<sub>6</sub>(TMEDA) in 100 mL of MeCN with 1.2 mL (1.0 g, 5.7 mmol) of PMDETA. After being heated at reflux for 1 h, the mixture was filtered to remove elemental sulfur and the filtrate was concentrated to ~5 mL. Orange-yellow crystals were collected and washed with 3 × 20 mL of Et<sub>2</sub>O. Yield: 1.82 g (93%).

**ZnS<sub>2</sub>C<sub>2</sub>(CO<sub>2</sub>Me)<sub>2</sub>(PMDETA) (3).** A solution of 0.250 g (0.681 mmol) of ZnS<sub>4</sub>(PMDETA) in 50 mL of MeCN was treated with 85 μL (98 mg, 0.69 mmol) of DMAD. The reaction solution immediately assumed a dark red color, and an off-white precipitate (sulfur) formed. After 1 h, the solution was filtered, and the filtrate was concentrated to 10 mL and then diluted with 50 mL of Et<sub>2</sub>O. The crude red precipitate was recrystallized by dissolution in 5 mL of Me<sub>2</sub>CO followed by treatment with 25 mL of Et<sub>2</sub>O to give pale white microcrystals. Yield: 0.262 g (86%). Anal. Calcd for C<sub>15</sub>H<sub>29</sub>N<sub>3</sub>O<sub>4</sub>S<sub>2</sub>Zn: C, 40.49; H, 6.57; N, 9.44; S, 14.41; Zn, 14.70. Found: C, 40.46; H, 6.85; N, 9.69; S, 14.20; Zn, 14.93. <sup>1</sup>H NMR (CD<sub>3</sub>CN), δ: 3.58 (s, 6H, OCH<sub>3</sub>); 2.77 (m, 2H, CH<sub>2</sub>); 2.66 (m, 4H, CH<sub>2</sub>); 2.55 (m, 2H, CH<sub>2</sub>); 2.36 (s, 15H, NCH<sub>3</sub>). IR (KBr): 1705 and 1667 cm<sup>-1</sup> (ν<sub>C=O</sub>).

**ZnS<sub>2</sub>C<sub>2</sub>(CO<sub>2</sub>Me)H(PMDETA) (4).** A solution of 0.250 g (0.681 mmol) of ZnS<sub>4</sub>(PMDETA) in 50 mL of MeCN was treated with 65 μL (61 mg, 0.73 mmol) of methyl propiolate. The reaction solution assumed a dark red color in 1 h, and an off-white precipitate (sulfur) formed. After 12 h, the solution was filtered, and the filtrate was concentrated to 10 mL and then diluted with 50 mL of Et<sub>2</sub>O. The crude orange precipitate was recrystallized by dissolution in 5 mL of Me<sub>2</sub>CO followed by treatment with 25 mL of Et<sub>2</sub>O to give a pale orange powder. Yield: 0.262 g (86%). Anal. Calcd for C<sub>13</sub>H<sub>27</sub>N<sub>3</sub>O<sub>2</sub>S<sub>2</sub>Zn: C, 40.36; H, 7.03; N, 10.86; S, 16.58; Zn, 16.90. Found: C, 39.92; H, 6.91; N, 9.61. <sup>1</sup>H NMR (CD<sub>3</sub>CN), δ: 7.91 (bs, 1H, CH); 3.59 (s, 3H, OCH<sub>3</sub>); 2.77 (m, 2H, CH<sub>2</sub>); 2.66 (m, 4H, CH<sub>2</sub>); 2.55 (m, 2H, CH<sub>2</sub>); 2.37 (s, 3H, NCH<sub>3</sub>); 2.34 (s, 12H, NCH<sub>3</sub>). IR (KBr): 1690 cm<sup>-1</sup> (ν<sub>C=O</sub>).

**ZnS<sub>3</sub>CS(PMDETA) (5).** A solution of 2.00 g (5.45 mmol) of ZnS<sub>4</sub>(PMDETA) in 100 mL of MeCN was treated with 0.500 mL (8.32 mmol) of CS<sub>2</sub>. The reaction solution immediately changed from a pale yellow to a dark gold color. After 1 h, a copious amount of an off-white solid (sulfur) had precipitated. The solution was stirred for 16 h, and then the precipitate was filtered off. The filtrate was evaporated, and the bright yellow residue was transferred to a Soxhlet thimble and extracted with CS<sub>2</sub> for 18 h. Yield: 1.75 g (85%). Anal. Calcd for C<sub>10</sub>H<sub>23</sub>N<sub>3</sub>S<sub>4</sub>Zn: C, 31.69; H, 6.12; N, 11.09; S, 33.85; Zn, 16.90. Found: C, 31.65; H, 6.25; N, 11.07; S, 33.00; Zn, 16.90. <sup>1</sup>H NMR (acetone-*d*<sub>6</sub>), δ: 3.12 (m, 2H, CH<sub>2</sub>); 2.86 (m, 4H, CH<sub>2</sub>); 2.75 (m, 2H, CH<sub>2</sub>); 2.50 (s, 12H, CH<sub>3</sub>); 2.47 (s, 3H, CH<sub>3</sub>). IR (KBr): 995 cm<sup>-1</sup> (ν<sub>C=S</sub>).

**ZnS<sub>2</sub>CS(PMDETA) (6).** A solution of 100 mg of ZnS<sub>3</sub>CS(PMDETA) (0.264 mmol) in 50 mL of MeCN was treated with 70 mg (0.267 mmol) of PPh<sub>3</sub>. The reaction solution was stirred for 16 h. The volume was reduced to ~20 mL, and an off-white precipitate (SPPH<sub>3</sub>) was filtered off. The filtrate was concentrated to ~5 mL and then diluted with 25 mL of Et<sub>2</sub>O to give yellow microcrystals. Yield: 75 mg (82%). Anal. Calcd for C<sub>10</sub>H<sub>23</sub>N<sub>3</sub>S<sub>3</sub>Zn: C, 34.62; H, 6.68; N, 12.11; S, 27.73; Zn, 18.85. Found: C, 34.46; H, 7.00; N, 11.75; S, 27.65; Zn, 19.12. <sup>1</sup>H NMR (CD<sub>3</sub>CN), δ: 2.81 (b m, 8H, CH<sub>3</sub>, CH<sub>2</sub>); 2.76 (m, 4H, CH<sub>2</sub>); 2.64 (m, 2H, CH<sub>2</sub>); 2.45 (b s, 6H, CH<sub>3</sub>); 2.23 (s, 3H, CH<sub>3</sub>). IR (KBr): 973 cm<sup>-1</sup> (ν<sub>C=S</sub>).

**Zn(S<sub>2</sub>C<sub>2</sub>S<sub>2</sub>CO)(PMDETA) (7).** A solution of 0.200 g of ZnS<sub>4</sub>(PMDETA) (0.545 mmol) in 50 mL of MeCN was treated with 0.115 g (0.552 mmol) of TPD. After 16 h, the reaction mixture assumed a purple color. A pale white precipitate (sulfur) was filtered off, and the filtrate was concentrated to ~10 mL and then diluted with 50 mL of Et<sub>2</sub>O. A purple-brown precipitate was filtered off and washed with 10 mL of CS<sub>2</sub> (to remove the purple impurity) and then 3 × 10 mL of Et<sub>2</sub>O to afford a tan-brown powder. Yield: 0.201 g (80%). Anal. Calcd for C<sub>12</sub>H<sub>23</sub>N<sub>3</sub>O<sub>5</sub>S<sub>4</sub>Zn: C, 34.40; H, 5.53; N, 10.03. Found: C, 34.25; H, 5.57; N, 9.99. <sup>1</sup>H NMR (CD<sub>3</sub>CN), δ: 2.78 (m, 2H, CH<sub>2</sub>); 2.68 (m, 4H, CH<sub>2</sub>); 2.57 (m, 2H, CH<sub>2</sub>); 2.42 (s, 12H, CH<sub>3</sub>); 2.30 (s, 3H, CH<sub>3</sub>). IR (KBr): 1660 and 1594 cm<sup>-1</sup> (ν<sub>C=O</sub>).

**Crystal Preparation and Structure Refinement Summary for ZnS<sub>4</sub>(PMDETA).** X-ray-quality crystals were grown from diffusion

of Et<sub>2</sub>O into a CH<sub>3</sub>CN solution of **1**. The data crystal was mounted using oil (Paratone-N, Exxon) onto a thin glass fiber. The sample was bound by faces (001), (00 $\bar{1}$ ), (010), (0 $\bar{1}$ 0), (110), ( $\bar{1}$ 10), ( $\bar{1}$ 10), ( $\bar{1}$ 10), and ( $\bar{1}$ 52). Distances from the crystal center to these facial boundaries were 0.360, 0.360, 0.140, 0.140, 0.160, 0.160, 0.180, 0.180, and 0.120 mm, respectively. Crystal and refinement details are given in Table 2. Systematic conditions suggested the space group  $P2_12_12_1$ . Standard intensities monitored during frame collection showed no decay. Intensity data were reduced by 3d-profile analysis using SAINT<sup>24</sup> and corrected for Lorentz–polarization effects and for absorption. Scattering factors and anomalous dispersion terms were taken from standard tables.<sup>25</sup> The structure was solved by direct methods;<sup>26</sup> the correct positions of Zn and S atoms were deduced from a vector map. Subsequent cycles of isotropic least-squares refinement followed by an unweighted difference Fourier synthesis revealed positions for the remaining non-H atoms. Methyl H atom positions, were optimized by rotation about N–C bonds with idealized C–H and H $\cdots$ H distances. Remaining H atoms were included as fixed idealized contributors. Methylene H atom  $U$ 's were assigned as 1.5 times  $U_{\text{eq}}$  and methyl H atoms  $U$ 's were assigned or 1.2 times  $U_{\text{eq}}$  of adjacent C atoms. Non-H atoms were refined with anisotropic thermal coefficients. Successful convergence of the full-matrix least-squares refinement<sup>27</sup> on  $F^2$  was indicated by the maximum shift/error for the last cycle. The highest peaks in the final difference Fourier map were in the vicinity of the Zn and S atoms; the final map had no other significant features. A final analysis of variance between observed and calculated structure factors showed no dependence on amplitude or resolution.

**Crystal Preparation and Structure Refinement Summary for ZnS<sub>2</sub>C<sub>2</sub>(CO<sub>2</sub>Me)<sub>2</sub>(PMDETA).** X-ray-quality crystals were grown from diffusion of Et<sub>2</sub>O into a CH<sub>3</sub>CN solution of **3**. The data crystal was

mounted using oil (Paratone-N, Exxon) onto a thin glass fiber. The sample was bound by faces (0 $\bar{1}$ 1), (011), (0 $\bar{1}$ 1), ( $\bar{1}$ 2 $\bar{1}$ ), (10 $\bar{1}$ ), and ( $\bar{1}$ 01). Distances from the crystal center to these facial boundaries were 0.060, 0.060, 0.075, 0.075, 0.115, and 0.115 mm, respectively. Crystal and refinement details are given in Table 2. Systematic conditions suggested the space group  $P2_1/n$ . Standard intensities monitored during frame collection showed no decay. Intensity data were reduced by 3d-profile analysis using SAINT and corrected for Lorentz–polarization effects and for absorption. Scattering factors and anomalous dispersion terms were taken from standard tables.<sup>24</sup> The structure was solved by direct methods; the correct positions of Zn and S atoms were deduced from a vector density map. Subsequent cycles of isotropic least-squares refinements followed by an unweighted difference Fourier synthesis revealed positions for the remaining non-H atoms. Methyl H atom positions were optimized by rotation about N–C bonds with idealized C–H and H $\cdots$ H distances. Remaining H atoms were included as fixed idealized contributors. Methylene H atom  $U$ 's were assigned as 1.5 times  $U_{\text{eq}}$  and methyl H atoms  $U$ 's were assigned 1.2 times  $U_{\text{eq}}$  of adjacent C atoms. Non-H atoms were refined with anisotropic thermal coefficients. Successful convergence of the full-matrix least-squares refinement on  $F^2$  was indicated by the maximum shift/error for the last cycle. The highest peaks in the final difference Fourier map were in the vicinity of the N, Zn, and S atoms; the final map had no other significant features. A final analysis of variance between observed and calculated structure factors showed no dependence on amplitude or resolution.

**Acknowledgment.** This research was supported by the National Science Foundation. We thank Atul Verma for assistance in the early stages of this project.

**Supporting Information Available:** Tables listing crystallographic data and structure refinement details, bond lengths, bond angles, anisotropic displacement parameters, and all atom coordinates for structures **1** and **3** (10 pages). Ordering information is given on any current masthead page.

IC971564F

(24) SAINT V4 and SHELXTL V5: Siemens Industrial Automation, Inc. Madison, WI, USA.

(25) *International Tables for X-ray Crystallography*; Wilson, A. J. C., Ed.; Kluwer Academic Publishers: Dordrecht, The Netherlands, 1992; Vol. C: (a) scattering factors, pp 500–502; (b) anomalous dispersion corrections, pp 219–222.

(26) Sheldrick, G. M. *Acta Crystallogr.* **1990**, A46, 467.

(27) Sheldrick, G. M. In preparation for *J. Appl. Crystallogr.*